Local random configuration-tree theory for string repetition and facilitated dynamics of glass

Chi-Hang Lam[1, *]

[1] *Department of Applied Physics, Hong Kong Polytechnic University, Hong Kong, China*

(Dated: July 10, 2017)

We derive a microscopic theory of glassy dynamics based on the transport of voids by micro-string motions, each of which involves particles arranged in a line hopping simultaneously displacing one another. Disorder is modeled by a random energy landscape quenched in the configuration space of distinguishable particles. We study the evolution of local regions with m coupled voids. At low temperature, energetically accessible local particle configurations can be organized into a random tree with nodes and edges denoting configurations and micro-string propagations respectively. A micro-string propagation initiated by a void can facilitate similar motions by other voids via perturbing the random energy landscape. Dynamics is dominated by coupled voids of an optimal group size, which increases as temperature decreases. We obtain explicit expressions of the particle diffusion coefficient and a particle return probability, which describe glassy behaviors at low temperature and small void density. Comparison with a distinguishable-particle lattice model (DPLM) of glass shows very good quantitative agreements using only a single adjustable parameter related to the interaction range of the micro-strings.

I. INTRODUCTION

The nature of the glassy state is one of the most fundamental and long-standing problems in the study of condensed matters [1–4]. The mechanism of a dramatic slowdown of the dynamics as the temperature T decreases is highly controversial, despite intensive efforts based on approaches such as the Adam-Gibbs theory [5], mode-coupling theory [6], random first order transition theory [7], dynamic facilitation theory [8–11] and so on.

A remarkable feature of glassy dynamics is a string-like particle hopping motion, in which neighboring particles arranged in a line displaces one another. It has been found to dominate particle dynamics in many glassy systems as observed in MD simulations [12–14] and experiments [15]. If particles in a string hop simultaneously, the motion is referred to as coherent. A coherent string or a coherent segment in a string is called a micro-string [14]. Recently, we have conducted MD simulations [16] of a bead-spring model of polymers and observe that string-like motions become highly repetitive at low T. This is directly related to back-and-forth particle hopping motions widely studied [17–22]. A return probability of hopped particles for simulated polymers studied in Ref. [16] reaches 73% at low T at equilibrium and it is even higher for non-equilibrium samples quenched to even lower T. Equilibration of quenched samples show further increase in the return probability. The simulation results indicate that as T decreases the return probability approaches towards unity, implying significantly slowed down dynamics. Examinations of particle trajectories show that those strings spatially isolated from other strings tend to repeat for much longer durations. A string typically breaks free of repetitions via a pair interaction with another string, realizing facilitated dynamics of strings.

Lattice models also play important roles in the study of glass and are often more tractable analytically [8, 9, 23–26]. We have proposed a distinguishable-particle lattice model (DPLM) of glass [27] to further study the string repetition and string interaction phenomena observed in MD simulations in Ref. [16]. The DPLM is a lattice gas model with infinite particle types generalizing an identical-particle sliding block model of glass [28]. It is closely related to lattice models of glass with particles of a few [25] or many types [29, 30], and is also related to many-species molecular models [31–33]. Typical glassy dynamics are demonstrated for a wide range of temperature and particle density. Defined by a simple Hamiltonian without explicit kinetic constraint except for simple particle exclusion, it exhibits emergent facilitation behaviors and may thus provide microscopic justifications for kinetic constraints assumed in kinetically constrained models (KCM) [8–11]. In addition, DPLM simulations reproduce the convergence of particle return probability towards unity as T decreases, analogous to that observed in MD simulations [16]. An additional property important to the present work is that equilibrium statistics are exactly known, rendering it as analytically tractable as the more coarse-grained models such as the KCM's.

In this paper, we describe the dynamics observed in polymer or DPLM simulations based on micro-strings in the presence of a random energy landscape in the particle configuration space. A random-tree theory is proposed and it provides particle diffusion coefficient characteristic of liquid and glass at high and low T respectively. We expect that the theory is generally applicable to glassy systems exhibiting string-like motions including polymer and DPLM simulations. Nevertheless, since required model parameters are reliably available only for the DPLM, we compare the theory quantitatively only to DPLM simulations. We demonstrate that using only

* Email: C.H.Lam@polyu.edu.hk

a single adjustable parameter, analytic results from the random tree theory are in good agreement with DPLM simulation data from Ref. [27].

The rest of this paper is organized as follows. Section II explains and further analyzes the DPLM. Section III describes both polymer and DPLM simulations on the same footing based on micro-strings. We formulate a random tree theory for a local region with a single void in Sec. IV. Our main results are then obtained by generalizations to include void coupling effects in local regions with multiple voids in Sec. V. Limiting cases for the liquid and glass phases are further studied in Sec. VI. Section VII concludes the paper with a summary.

II. DISTINGUISHABLE-PARTICLE LATTICE MODEL (DPLM)

Following Ref. [27], the DPLM is defined in $d = 2$ dimensions with N particles on a $L \times L$ square lattice following periodic boundary conditions. It is an interacting lattice gas model with distinguishable particles. No more than one particle can occupy a site. If site i is occupied, the particle index $s_i = 1, 2, \ldots, N$ specifies which particle occupies the site. Otherwise, $s_i = 0$ and the site is occupied by a void. The system energy is

$$E = \sum_{<i,j>'} V_{ijs_is_j} \tag{1}$$

where the sum is over occupied nearest neighboring (NN) sites.

An important feature of the DPLM is the site-particle dependent interaction V_{ijkl}, which depends on both the sites i and j and the particle indices k and l. Each V_{ijkl} follows an *a priori* distribution $g(V)$ taken as the uniform distribution in $[-0.5, 0.5]$, i.e.

$$g(V) = \begin{cases} 1, & \text{for } -0.5 \le V \le 0.5 \\ 0, & \text{otherwise.} \end{cases} \tag{2}$$

Note that the interaction $V_{ij}(t) \equiv V_{ijs_is_j}$ at site i and j for arbitrary particles admits an implicit time dependence via s_i and s_j, which change in value when a particle at i or j is replaced. Hence, the disorder is not quenched in the physical space. In contrast, since each V_{ijkl} is a quenched random value for any given particles k and l, the interaction is fixed for any given local particle configuration. The disorder is therefore quenched in the configuration space instead.

The dynamics follow standard kinetic Monte Carlo rules. Each particle can hop to an unoccupied NN site at a rate

$$w = w_0 \exp\left(-\frac{E_0 + \Delta E/2}{k_B T}\right) \tag{3}$$

where ΔE is the change in the system energy E due to the hop. We also choose $E_0 = 1.5$ and $w_0 = 10^6$ following Ref. [27].

Kinetic Monte Carlo simulations of the DPLM using Eq. (3) for a wide range of T and void density ϕ_v show no sign of undesired crystalization or particle segregation. At high T or large ϕ_v, behaviors typical of simple non-glassy fluids are observed. By contrast, at low T and small ϕ_v, one observes typical behaviors of glass including a plateau in the mean square displacement (MSD), a super-Arrhenius T dependence of the particle diffusion coefficient D, a self-intermediate scattering function decaying stretched-exponentially towards zero at long time, a violation of the Stokes-Einstein relation, and an increasing four-point susceptibility as T decreases.

For small void density ϕ_v, the particle diffusion coefficient D at any given T exhibits the scaling relation

$$D \sim \phi_v^{\alpha}. \tag{4}$$

At high T, $\alpha \simeq 1$ indicating particle motions induced by independent void motions. As T decreases, α rises monotonically. For $\alpha \simeq 2$ for instance, $D \sim \phi_v^2$ corresponds to motions dominated by coupled pairs of voids while single voids are trapped. This demonstrates emergent facilitated dynamics of voids.

A feature crucial to this work is that equilibrium statistics of the DPLM is known exactly. For any given configuration, we refer to an interaction $V_{ijs_is_j}$ which directly appears in the energy function in Eq. (1) as realized, and V_{ijkl} as unrealized if particle k and l are not currently located at site i and j respectively. At equilibrium, an unrealized interaction V_{ijkl} simply follows the *a priori* distribution $g(V_{ijkl})$ in Eq. (2). In contrast, a realized interaction $V_{ijs_is_j}$ follows a posteriori distribution

$$p_{eq}(V_{ijs_is_j}) = \frac{1}{\mathcal{N}} e^{-\beta V_{ijs_is_j}} g(V_{ijs_is_j}) \tag{5}$$

where $\mathcal{N} = \int e^{-\beta V} g(V) dV$ is a normalization constant and $\beta = 1/k_B T$ with $k_B = 1$ being the Boltzmann constant. The distribution g is thus analogous to a density of state and it is being weighted by the Boltzmann factor in Eq. (5).

We now further analyze the DPLM theoretically. We describe a particle hop equivalently as the hop of a void in the opposite direction. For a hop attempt of an isolated void to an occupied NN site, Eq. (1) implies an energy change of the system given by

$$\Delta E = \sum_{\gamma=1}^{3} (V'_\gamma - V_\gamma), \tag{6}$$

where V_γ denotes the three realized interactions following p_{eq} to be broken, while V'_γ denotes the three prospective interactions following g to be realized. We obtain the probability distribution $P(\Delta E)$ of ΔE by numerically performing the convolution of the six distributions from Eqs. (2) and (5) of these six random variables.

To allow further analysis, we consider a hop attempt energetically possible if

$$\Delta E \le k_B T. \tag{7}$$

Otherwise, it is deemed unlikely and neglected. The probability q that an allowed hop is energetically possible follows

$$q = \int_{-\infty}^{k_B T} P(\Delta E) d\Delta E. \tag{8}$$

As T decreases, q decreases monotonically from 1 to 0.

Denote the coordination number of the square lattice used in the DPLM by $z_0 = 4$. Let z be the number of possible hops an isolated void is allowed to make. Since only nearest neighboring hops are allowed, $z = z_0 = 4$. However, on average only zq of the z allowed hops are energetically possible. At equilibrium, excitation and de-excitation events must be balanced so that ΔE averages to 0. Most hops following Eq. (7) thus also follows $\mid \Delta E \mid \leq k_B T$. Neglecting ΔE in Eq. (3), the rates of all energetically possible hops are approximated by the uniform rate

$$\tilde{w} = w_0 \exp(-E_0/k_B T). \tag{9}$$

This also implies the assumption of a uniform energy for all energetically accessible configurations. Similar to MD and DPLM simulations, the simplified dynamics defined here follows detailed balance.

III. MICRO-STRINGS, VOIDS AND DISTINGUISHABLE PARTICLES

During a string-like motion, each particle arranged in a line of particles hops to displace the preceding one [12]. If particles in a string hop simultaneously, it is referred to as a coherent string or a micro-string [14]. A string, typically a longer one, can be incoherent and consists of a number of micro-strings. The coherent hops of particles in a micro-string can be energetically preferred [34] because particle bonds within the micro-string need not be broken. Micro-strings are usually very short and their average length $\tilde{l}$ is less than 2 particles long, as it is bounded by the average length of strings [13]. The structural feature allowing a micro-string motion has been proposed as an elementary excitation in glassy systems [35]. On the other hand, free volumes are long known to be important for glassy dynamics [36]. Motivated by the observation of highly repetitive particle hops dominated by hopping distances comparable to the particle diameter, we have suggested that the existence of a void of a free volume comparable to that of a particle is the elementary excitation allowing a micro-string [16]. In this paper, we follow Ref. [16] and assume that a micro-string must involve a void and the propagation of a micro-string transport its void from one end of the micro-string to the other. More precisely, such a void is a quasi-particle transported by a micro-string in whole, but can be fragmented and distributed among a few interstitial volumes before and after a hop. This may reconcile with the fact that contiguous voids or free volumes have been found to show only small correlations with particle motions [37–39].

For the DPLM, the above picture of particle motions based on voids and micro-strings is also applicable. Voids exist and participate in particle motions by definition. Since particles perform independent single hops, each hop constitutes a micro-string of unit length implying an average micro-string length of $\tilde{l} = 1$ particle.

Conversely, quantitative measures developed for the DPLM in Sec. II can also be generalize to molecular systems with dynamics dominated by string-like motions. Specifically, we define q as the probability that an allowed micro-string is energetically possible so that it varies from 1 to 0 as T decreases. Also, we define zq as the average number of energetically possible micro-strings executable by a void. Then, z can be interpreted as the average number of geometrically allowed micro-strings limited to within a commonly observed micro-string length, say up to about 3 particles long [14]. It may then relates to the particle coordination number z_0 in the physical space very roughly as $z \sim z_0^3$.

Analogous to Eq. (9), we also assume in general for simplicity that all energetically possible micro-strings have a uniform propagation rate $\tilde{w}$. This effectively also assumes a uniform energy of all configurations in the random tree.

Throughout this work, we will consider distinguishable particles. For the DPLM, particles are distinguishable by definition. For molecular systems, examples like polydisperse hard disks and monomers in polymer chains also admit distinct particle properties in general and this justifies the distinguishability. For other glasses especially monoatomic ones, it is less trivial. It may describe the fact that different particles, upon hopping into a void, in general lead to different frustrations and hence different interaction energies, analogous to the distinguishable particle case.

IV. RANDOM TREE THEORY FOR ISOLATED VOIDS

In this and the next session, we develop a theory of glassy dynamics based on micro-string motions applicable to both molecular systems and the DPLM. Consider a d-dimensional physical space, where d=2 or 3 . Volumes in the followings are implied to be d-dimensional volumes. Let ϕ and ϕ_v be the density of particles and voids respectively. The average volume Ω of a particle and of a void follows

$$1/\Omega = \phi + \phi_v. \tag{10}$$

Consider a local region of volume $\mathcal{V}$ with a single isolated void. More details about the definition of such a region will be discussed in Sec. V. A local configuration specifies the positions of all distinguishable particles in the region. The set of all possible configurations constitutes the configuration space, which can be organized as a graph [40] by defining nodes as configurations and

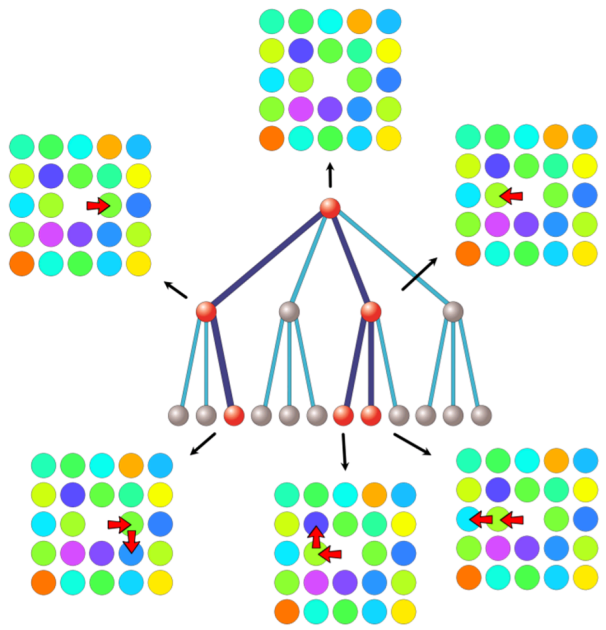

FIG. 1. The first three levels of a Bethe lattice representing the configuration space of a local region with a single void in the DPLM. Each node denotes a particle configuration of the region. An edge joins two configurations connected by an allowed micro-string propagation, corresponding to a hop of a particle or equivalently of a void. The coordination number z of the Bethe lattice equals the coordination number $z_0 = 4$ of square lattice representing the physical space. Starting from a local particle configuration associated with the root, void motions (red arrows) leading to 5 examples of descendent nodes are illustrated. Particles are randomly colored to highlight their distinguishability. The propagation of a micro-string may be energetically possible (dark blue) with a probability q. The energetically accessible nodes (red spheres) form a local random configuration tree. The random tree shown is illustrated for e.g. $q = 0.5$ so that its average degree is $c_1 = 1.5$.

edges connecting pairs of configurations related by allowed micro-string propagations. Figure 1 shows an example of such a configuration graph for the DPLM describing a 5×5 region with a single void. The graph has been further arranged as a tree and only the first three levels are shown. The root, defined as level 0, is statistically equivalent to any other nodes and can be used to represent any given configuration. In this example, it is associated with a configuration with the void at the center. It is directly connected to 4 nodes in the first level and further to 12 nodes at the second level corresponding to all possible single and double hops of the void respectively.

As explained in Sec. III, we assume particle distinguishability. A configuration thus specifies not only the position of the void but also the positions of all particles. An important consequence is illustrated in Fig. 2 for the same DPLM example, in which configurations (b) and (c) have the same void position. For identical particle systems, they represent identical configurations with an equal energy. The two corresponding nodes are then identical and can be merged together leading to a loop. The tree geometry is then a very rough approximation. In sharp contrast, due to particle distinguishability, configurations (b) and (c) are different because three particles are located differently. In fact, all 12 nodes in the second level are distinct and the tree structure represents the exact geometry of the graph so far.

Each node in the configuration graph is directly connected to z edges, where z denotes the number of allowed micro-strings executable by a void as explained in Sec. III, Neglecting loops, the configuration graph takes the geometry of a Bethe lattice with a coordination number z. For the DPLM, the Bethe lattice exactly represents the configuration graph for up to the 5th tree-level, only beyond which loops occur. This is because for a 2×2 block with a void and three particles, 6 consecutive hops of the void in the clockwise direction is the least required to arrive at the same configuration resulting from 6 analogous hops of the void in the anti-clockwise direction. Equivalently, 12 consecutive hops of the void return the region to the original configuration as each of the three particles would have hopped four times and returned to their original positions. The Bethe lattice is thus a very good approximation for the single void case. We emphasize that the Bethe lattice approximates the configuration space rather than the d-dimensional physical space.

It is tempting to consider the dynamics as a random walk of the void in the d-dimensional physical space with a random energy landscape. However, this is not appropriate for distinguishable-particle systems because the void position does not uniquely determine the system energy E. For DPLM, this is evident from Eq. (1). Furthermore, configurations (b) and (c) in Fig. 2 have the same void position but are in fact distinct because 3 particles are located differently. Their energies are in general different with seven of the interactions $V_{ijs_is_j}$ (indicated by short black lines) distinct. For distinguishable-particle systems in general, the system energy E depends on the detailed particle configurations. The dynamics is thus a random walk of the configuration in a random energy landscape defined in the configuration space rather than in the d-dimensional physical space.

Denote the current particle configuration by the root of the Bethe lattice without loss of generality. We classifying allowed micro-strings as energetically possible or impossible with probabilities q and $1 - q$ respectively as explained in Sec. III. The root is then only connected to a random sub-tree of the Bethe lattice separated from other nodes by idealized insurmountable energy barriers. An example of a random tree is illustrated in Fig. 1.

This local random configuration tree of energetically accessible nodes is our main focus of study. The average number of children of each node is

$$c_1 = (z - 1)q, \tag{11}$$

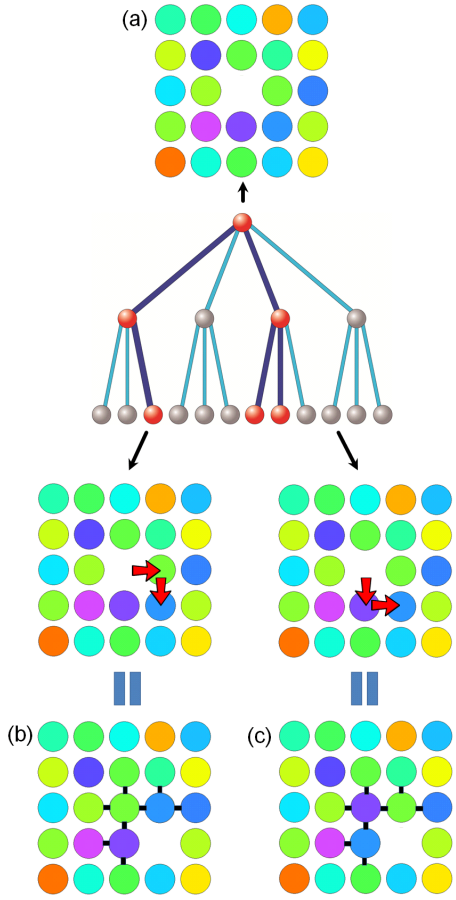

FIG. 2. The same Bethe lattice and random tree for the DPLM as in Fig. 1. Starting from configuration (a) denoted by the root, two hops of the void in clockwise direction results at configuration (b). Alternatively, two hops in anti-clockwise direction lead to a different configuration (c), with 3 particles located differently and 8 interactions different (black lines) despite an identical void position.

except for the root which has on average zq children. Here, c_1 is called the average degree, noting that the tree is approximately an Erdös-Rényi random graph, also called a Poisson random graph [40].

As T decreases, q decreases monotonically from 1 to 0 as explained in Sec. III and Eq. (11) implies that c_1 decreases from $z-1$ to 0. Noting that $z=4$ for the DPLM and it is expected to be larger for molecular systems, we have $z \gg 1$. There must exist a temperature T_1 at which $q = 1/(z-1)$ so that $c_1 = 1$. For $T < T_1$ so that $c_1 < 1$, it is straightforward to show that the random tree must be finite with on average $N_{tree} = (1+q)/(1-c_1 q)$ nodes. For $T \geq T_1$ so that $c_1 \geq 1$, the tree can be infinite and the average number of nodes N_{tree} diverges, i.e.

$$N_{tree} = \begin{cases} \infty, & \text{for } \ c_1 \geq 1 \\ \dfrac{1+q}{1-c_1 q}, & \text{for } \ 0 < c_1 < 1. \end{cases} \tag{12}$$

To describe the dynamics of a local region with a single void, we will consider the following equivalent pictures:

1. random walk of the configuration in the random tree, characterized by the net level transcending rate μ;
2. random walk of the void in the physical space, characterized by net hopping rate R_{void} of the void;
3. random walks of the particles in the physical space, characterized by the particle diffusion coefficient D_1.

Below, We will calculate μ, R_{void} and hence D_1.

First, we study the random walk of the configuration in the random tree. Note that all edges corresponding to energetically possible micro-string propagations are assumed the uniform rate $\tilde{w}$ for simplicity as explained in Sec. III. The quenched disorder in the configuration space is thus encoded only as kinetic constraints on the Bethe lattice and realized as the geometry of an energetically trivial random tree. These simplifications are analogous to those in KCM [11].

The random walk of the configuration is thus a simple unbiased random walk in the random tree. For $T > T_1$ so that $c_1 > 1$, the random tree can be infinite according to Eq. (12). Beyond the root, the rate of a level-decreasing hop is $\tilde{w}$, while that of a level-increasing hop is on average $c_1\tilde{w}$. Neglecting the different rates at the root which is irrelevant at long time, the level transcending rate, defined as the net rate of increase in the level, is $\mu = (c_1 - 1)\tilde{w}$ [41]. For $T \leq T_1$ so that $c_1 \leq 1$, the tree is finite according to Eq. (12). On average, the level first increases from 0 before being saturated with $\mu = 0$. At long time, there are indefinite recurrence of the N_{tree} configurations and indefinite back-and-forth repetitions of the $N_{tree} - 1$ micro-strings. Summarizing, we have

$$\mu = \begin{cases} (c_1 - 1)\tilde{w}, & \text{for } \ c_1 \geq 1. \\ 0, & \text{for } \ 0 < c_1 < 1 \end{cases} \tag{13}$$

Equation (13) shows an ideal mobile-to-immobile transition at $c_1 = 1$ applicable in the long-time limit. To understand the transition, consider c_1 decreasing towards 1 from above so that μ converges to 0 continuously. This corresponds to the infinite random tree becoming increasingly slim with a backbone converging to a one-dimensional geometry. The configuration mostly walks randomly back and forth with only an arbitrarily slight drift μ towards higher levels at long time. However, at shorter time, there is a finite drift $\mu > 0$ away from the root because the walk starts from the root and because the level cannot decrease further at the root [42]. A more accurate calculation should involve a time average of μ only up to the residence time of the void in the local region, which should turn the sharp transition into a smooth crossover.

Second, we project the random walk of the configuration into a random walk of the void. The tree-level transcending rate μ simply equals the net micro-string

propagation rate. Noting that each micro-string on average involves $\tilde{l}$ simultaneous hops by a void, the net hopping rate of the void is thus $R_{void} = \tilde{l}\mu$, Applying Eq. (13), we have

$$R_{void} = \begin{cases} \tilde{l}(c_1 - 1)\tilde{w}, & \text{for } \ c_1 \geq 1. \\ 0, & \text{for } \ 0 < c_1 < 1 \end{cases} \tag{14}$$

We emphasize that R_{void} calculated here is a net hopping rate accounting for the non-reversal parts of the random walk of the void. The back-and-forth parts are accounted for by the slow-down factor $c_1 - 1$ for $c_1 \geq 1$. The net motion of the void in the physical space is a non-reversal random walk which forbids backward retracing of the pathway. Nevertheless, it is not a self-avoiding walk. For example, the void can perform a loop and return to a previously visited position.

Finally, we study the motions of the particles as induced by those of the void. There are on average $\phi\mathcal{V}$ particles in the local region. Since each hop of the void is equivalent to a hop of a particle in the opposite direction, the net hopping rate per particle in the region is

$$R_{ptcle} = R_{void}/\phi\mathcal{V}. \tag{15}$$

Similarly, R_{ptcle} is also a net rate characterizing the non-reversal part of the particle random walk. The back-and-forth motions of the particles due to those of the void are excluded. Successive steps of the net motion of each particle are expected to be only slightly correlated. A subtle point is that a non-reversal walk of the void can induce reversed steps of particles. For example, the void can first induce a hop of a particle, perform a loop in the physical space, and the return to induce a second hop of the same particle in the opposite direction. This is not a reversal step of the void nor of the local particle configuration and it is not excluded. The net motion of the particle is thus neither a non-reversal nor a self-avoiding random walk.

We approximate the net motions of the particles by simple uncorrelated random walks, This is appropriate because the strongest correlation in the form of back-and-forth motions have been excluded. The particle diffusion coefficient in a single-void region is then $D_1 = a^2 R_{ptcle}/(2d)$, where a is the average particle hopping distance and is comparable to the particle diameter. Applying also Eqs. (14), (15) and (10), we get

$$D_1 = \begin{cases} \dfrac{(c_1 - 1)\tilde{l}\tilde{w}a^2\Omega}{2d(1 - \phi_v\Omega)\mathcal{V}}, & \text{for } \ c_1 \geq 1 \\ 0, & \text{for } \ 0 < c_1 < 1 \end{cases} \tag{16}$$

A dependence of D_1 on $\mathcal{V}$ may appears at a first sight unexpected for this single-void case. However, the physically relevant quantity is in fact the particle diffusion coefficient $\tilde{D}$ averaged over regions with non-interacting voids. Neglecting void interactions by neglecting regions with multiple voids, the probability that a region has a single void for small ϕ_v is $f(1, \phi_v\mathcal{V}) \simeq \phi_v\mathcal{V}$. Regions with no void have null contribution to diffusion. The particle diffusion coefficient $\tilde{D}$ averaged over all regions is hence $\tilde{D} = f(1, \phi_v\mathcal{V})D_1$, which simplifies to

$$\tilde{D} = \begin{cases} \dfrac{(c_1 - 1)\tilde{l}\tilde{w}a^2\phi_v\Omega}{2d(1 - \phi_v\Omega)}, & \text{for } \ c_1 \geq 1 \\ 0, & \text{for } \ 0 < c_1 < 1 \end{cases} \tag{17}$$

and is independent of $\mathcal{V}$. Equation (17) however neglects void interactions and generalizations leading to qualitatively different results will be explained next.

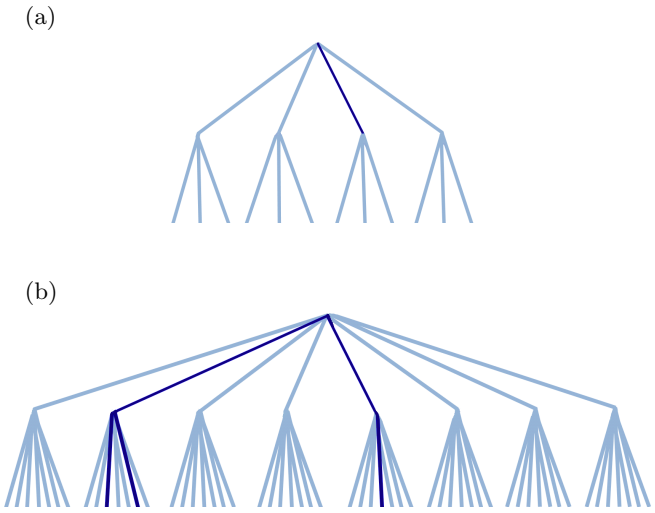

FIG. 3. (a) A simplified schematic diagram of the first three levels of a Bethe lattice (blue) and a random tree (dark blue) for a local region in the DPLM with a single void. The random tree is illustrated for, e.g. $q = 0.25$, so that the average degree is $c_1 = 0.75$ implying a finite tree. (b) A similar diagram for a local region with two voids also illustrated for $q = 0.25$. The average degree increases to $c_2 = 1.75$ and the random tree can be infinite.

V. RANDOM TREE THEORY FOR INTERACTING VOIDS

We have considered a single void associated with z allowed micro-strings, leading to a coordination number z of the Bethe lattice representing the configuration space. Figure 3(a) shows a schematic diagram of the Bethe lattice for the DPLM with $m = 1$ and $z = 4$, which is a simplified version of that in Fig. 1.

We now generalize our results to include local regions with $m \geq 2$ voids. With m voids, there are in general mz allowed ways that the local region can evolve via a single micro-string propagation by any of the m voids. After one of these micro-string propagates, there are again mz allowed micro-string propagations including the reversed one. A key issue is that some of these $mz - 1$ non-reversing micro-strings may not be new and this will be further discussed. Formally, we can still organize the

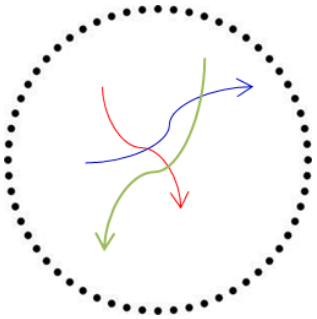

FIG. 4. A schematic diagram of a local region with 3 voids and 3 associated micro-strings which fully interact. The arrows show the pathways of voids during the propagation of the micro-strings. Due to the spatial overlaps, the propagation of any one of the micro-strings changes the energy landscape experienced by the other voids. The other two micro-strings are in general suppressed and on average two new micro-strings (not shown) are enabled. This enriches the configurations accessible by the dynamics and facilitates motions.

configuration space into a Bethe lattice with a coordination number mz, as illustrated in Figure 3(b) for the DPLM with $m = 2$ and $mz = 8$.

More precisely, some nodes in this Bethe lattice are identical, which upon merging lead to loops starting from the second level. For example, two voids far apart can each initiate a micro-string in arbitrary order and arrive at the same particle configuration, leading to two identical nodes at the second level. Without merging these nodes, the traversabilities of edges admit considerable correlations.

To minimize these correlations among edges, a region should have a small volume $\mathcal{V}$ so that voids within a region must be closeby to each other. This will be further explained later. Then, we can take the simple approximation that all voids in a region fully interact, i.e. every pair of micro-strings overlap spatially [16]. Figure 4 shows schematically a fully interacting set of micro-strings for $m = 3$ and $z = 1$, where an unphysically small z is chosen for ease of illustration. Denoting the current configuration by the root, the 3 micro-strings connects the root to 3 first-level nodes. The propagation of any of the micro-strings alters the particle configuration and the energy landscape so that the other two micro-strings are in general suppressed. Under equilibrium conditions, two new micro-strings on average are generated, leading to two new second-level nodes for each first-level node. This breaks the correlations among the edges of the Bethe lattice.

We thus assume that each edge in the Bethe lattice is independent of the others and is traversable with a probability q. The energetically accessible configurations is then a random subtree of the Bethe lattice with an average degree $c_m = (mz-1)q$. Applying Eq. (11), we can write $c_m = mc_1 + ((m-1)/(z-1))c_1$. Noting $z \gg 1$ for systems of interest, the second term is small. To simplify further algebra, we approximate c_m as

$$c_m = mc_1 = m(z-1)q. \tag{18}$$

Generalizing Eq. (16), the particle diffusion coefficient D_m in a region with $m \geq 1$ voids follows

$$D_m = \begin{cases} \dfrac{(c_m - 1)\tilde{l}\tilde{w}a^2\Omega}{2d(1-\phi_v\Omega)\mathcal{V}}, & \text{for } c_m \geq 1 \\ 0, & \text{for } 0 < c_m < 1. \end{cases} \tag{19}$$

An important consequence is that a larger group size m leads to larger c_m and D_m corresponding to a higher mobility. Denoting T at which $c_m = 1$ by $T = T_m$. For example for $T_2 < T < T_1$, one gets $c_2 > 1 > c_1$ so that a region with a single-void is in the immobile phase described by a finite random tree while a region with two voids is in the mobile phase described by an infinite random tree, as illustrated by Figs. 3(a) and (b) respectively.

Finally, voids are expected to have a uniform random spatial distribution, if aggregation is insignificant such as in the DPLM [27]. Then, the number of voids m in a region of volume $\mathcal{V}$ follows a probability distribution $f(m;\bar{m})$ which can be approximated by the Poisson distribution

$$f(m;\bar{m}) = \frac{\bar{m}^m e^{-\bar{m}}}{m!}. \tag{20}$$

with an average $\bar{m} = \phi_v\mathcal{V}$. Averaging over all regions, the particle diffusion coefficient is

$$D = \sum_{m=1}^{\infty} f(m;\phi_v\mathcal{V})D_m. \tag{21}$$

Using Eqs. (19) and (18), we finally get

$$D = \sum_{m>1/c_1} f(m;\phi_v\mathcal{V})\frac{(mc_1-1)\tilde{l}\tilde{w}a^2\Omega}{2d(1-\phi_v\Omega)\mathcal{V}}. \tag{22}$$

Equation (22) provides an explicit expression of D and is the main result of this work.

By using Eq. (20), we have implicitly assumed the simplest scenario that the physical space is statically partitioned into local regions each of volume $\mathcal{V}$. More precisely, we envision instead time-dependent local regions each of which moves and deforms dynamically following the void motions to encapsulate strongly coupled voids and to exclude farther ones not interacting with the group. This is motivated by the observation that a pair of voids can appear bounded together for extended period of time in DPLM simulations [27]. This picture of dynamic local regions should induce some quantitative deviations from Eq. (20) but should not alter our results qualitatively. From time to time, voids are exchanged between interacting groups and thus necessarily also between the dynamic local regions. We observe from DPLM simulations that this most often occurs when a

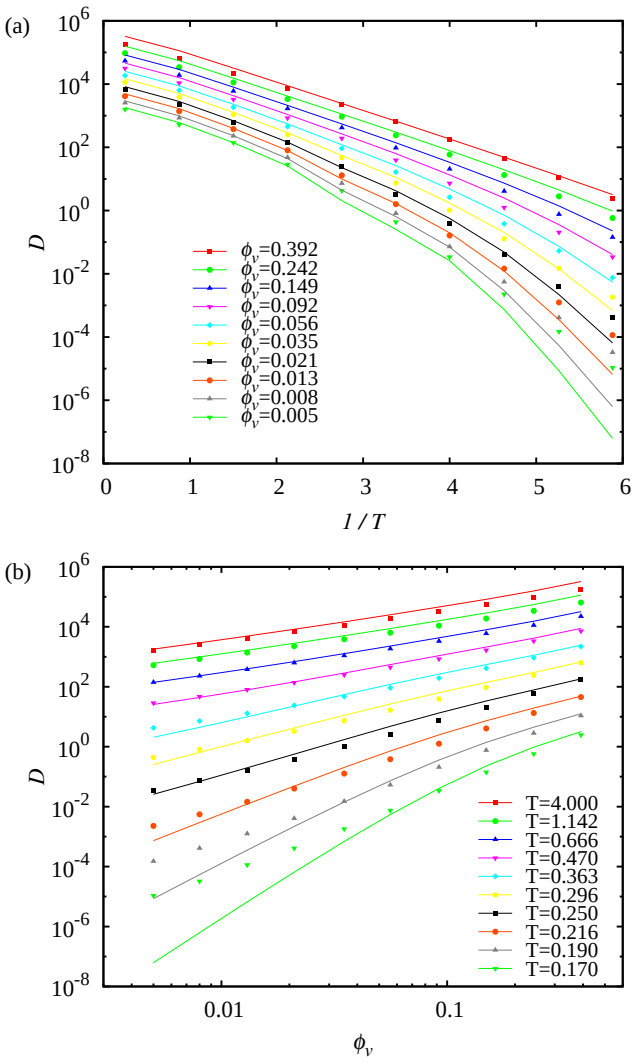

FIG. 5. Particle diffusion coefficient D against $1/T$ (a) and void density ϕ_v (b) for the DPLM from kinetic Monte Carlo simulations in Ref. [27] (symbols) and random-tree theoretical result in Eq. (22) (lines). The random-tree theory uses $\mathcal{V} = 25$, which is the only adjustable parameter.

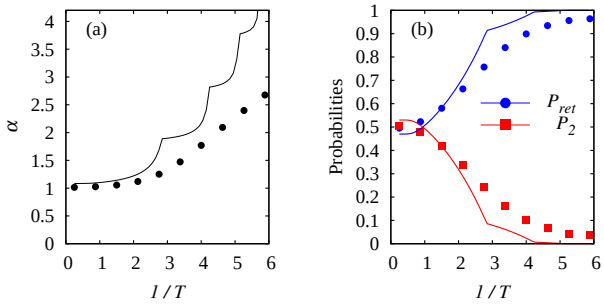

FIG. 6. Scaling exponent α (a), and probabilities of returning (P_{ret}) and non-returning (P_2) hops (b) against $1/T$ for the DPLM from kinetic Monte Carlo simulations in Ref. [27] (symbols) and random-tree theoretical results in Eqs. (22) and (25) (lines). The random-tree theory uses the same parameters as in Fig. 5 and has no additional adjustable parameter.

mobile group of m particles with $c_m > 1$ diffuses collectively around, picking up or dropping down individual voids. These void exchanges occur at longer time scale and are neglected in this work.

Equation (22) will now be checked against kinetic Monte Carlo simulations of the DPLM from Ref. [27]. Values of D measured from simulations are plotted as symbols in Figure 5(a) against $1/T$ for various ϕ_v. Figure 5(a) replots the same data set in the form of D against ϕ_v for various T. To apply our analytic expression in Eq. (22), note that most of the required parameters are exactly known: $d = 2$, $z = 4$, $a = \Omega = \tilde{l} = 1$, while q can be numerically calculated from Eq. (8). The only fitted parameter is $\mathcal{V} = 5^d = 25$. Using these parameters, fitted values of D calculated from Eq. (22) are plotted as lines in Figs. 5(a) and (b).

The good fits in Figs. 5(a) and (b) show that our analytic theory agrees very well with kinetic Monte Carlo simulations, especially for $D \gtrsim 10^{-2}$. In particular, two important qualitative features found in the simulations in Ref. [27] are successfully reproduced. First, from Fig. 5(a), D from Eq. (22) exhibits a crossover from an Arrhenius T dependence at large ϕ_v to a super-Arrhenius one at low ϕ_v. Second, from Fig. 5(b), the linear regions of the theoretical lines in the log-log plot for small ϕ_v verify the power-law in Eq. (4).

In Fig. 6(a), the symbols show the scaling exponent α defined in Eq. (4) measured from kinetic Monte Carlo simulations from Ref. [27]. We have also obtained theoretical values of α from the slopes of the theoretical lines of D versus ϕ_v in the log-log plot in Fig. 5(b). The result is plotted as a line in Figure 6(a). As seen, the theoretical result reproduces qualitatively the trend found in kinetic Monte Carlo simulations. In particular, the onset of the rise of α from 1 at $1/T \simeq 2.5$ is well reproduced.

We have suggested back-and-forth particle hops at low T as the main cause of kinetic arrest in glass [16, 27]. To study back-and-forth motions quantitatively, we monitor the subsequent motion of a particle after it has hopped to check if it first performs a returning hop to the original site or a genuine second hop to a new site. The two types of events contribute to the probabilities P_{ret} and P_2 respectively. Symbols in Fig. 6(b) shows P_{ret} and P_2 from kinetic Monte Carlo simulations of the DPLM from Ref. [27].

We now calculate P_{ret} and P_2 analytically. Consider a hopped particle labeled as k_0. Noting that a region with more voids generates proportionately more hops, particle k_0 resides at a region with m voids with probability $p_m \propto mf(m;\phi_v\mathcal{V})$. Since Poisson distribution satisfies

$$\sum_{m=0}^{\infty} mf(m;\phi_v\mathcal{V}) = \phi_v\mathcal{V}, \tag{23}$$

a normalization gives

$$p_m = mf(m;\phi_v\mathcal{V})/\phi_v\mathcal{V}. \quad (24)$$

Denote the configuration before the first hop by the root of the random tree without loss of generality. After the first hop, the configuration is at level 1 of the tree. Returning to the root implies a return hop of particle k_0. Alternatively, further ascending in level in the tree in general involves any of the $n_{\mathcal{V}} = \mathcal{V}/\Omega - m$ particles in the region. It may involve particle k_0 after visiting on average $n_{\mathcal{V}}/2\tilde{l}$ other distinct nodes on the tree. Since $n_{\mathcal{V}}/2\tilde{l} \gg 1$, this occurs practically at an infinite tree level. For a finite tree, this is impossible and particle k_0 can hence only return to the root contributing to P_{ret}. For an infinite tree, the configuration may first return to the root with a probability $1/c_m$ [42] and this contributes to P_{ret}. Otherwise, it goes to infinite level first with a probability $1 - 1/c_m$. The first edge encountered at a high tree-level involving particle k_0 pushes it to any of the z_0 NN sites, where z_0 is the average particle coordination number in the physical space already defined above. Particle k_0 may then accidentally reverse the original hop without reversing the regional configuration with a probability $1/z_0$ and contributes to P_{ret}. Otherwise, it may perform a new hop with probability $1 - 1/z_0$ and contributes to P_2. Putting all these together, particle k_0 first performs a new hop only for the case of an infinite tree, i.e. $c_m > 1$, with a probability $(1 - 1/z_0) \times (1 - 1/c_m)$. Averaging over regions with all possible values of m weighted by p_m in Eq. (24), we get

$$P_2 = \left(1 - \frac{1}{z_0}\right) \sum_{m>1/c_1} \frac{mf(m;\phi_v\mathcal{V})}{\phi_v\mathcal{V}} \left(1 - \frac{1}{mc_1}\right). \quad (25)$$

where Eq. (18) have been used. Also, P_{ret} follows from

$$P_{ret} = 1 - P_2. \quad (26)$$

We have calculated theoretical values of P_{ret} and P_2 using Eqs. (25) and (26) for the DPLM with $z_0 = z$ and the same parameters used above including $\mathcal{V} = 25$ determined in the previous fit to D. There is no adjustable parameter at all. The results are shown as lines in Figure 6(b). Good quantitative agreement between Eqs. (25)-(26) and kinetic Monte Carlo simulations is observed. In particular, the qualitative trend that $P_{ret} \to 1$ and $P_2 \to 0$ at low T suggested by data from both polymer [16] and DPLM simulations [27] is successfully reproduced. With no tunable parameter, the agreement obtained here is a highly non-trivially support of the validity of our theory for the DPLM.

Note that the theoretical values of α, P_{ret}, P_2 and in fact also D shown in Figs. 5(a), 6(a) and 6(b) are piecewise smooth functions of T. As T decreases, non-analyticities occur at $T = T_m$ at which $c_m = 1$ corresponding to $c_1 = 1/m$ for $m = 1, 2, 3, \ldots$. Physically, they corresponds to T at which regions with $m = 1, 2, 3, \ldots$ voids successively entering the immobile phase. The non-analyticity inherent from those in Eq. (13) and its m-void generalizations. It is an artifact expected to be smoothed out in more detailed calculations as already explained for Eq. (13).

As T decreases, dynamics are dominated by regions with $m = m^*$ voids in the mobile phase, as will be further explained in Sec. VI. The relevant local regions should hence have a volume $\mathcal{V}$ for encapsulating m^* coupled voids. We note that the interaction range of a void is of the order of the length of a micro-string plus a boundary layer which is roughly $(\tilde{l} + 2)a$. Thus, $\mathcal{V}$ is roughly of order $m^*(\tilde{l}+2)^d\Omega$, which increases as T decreases. A overly large $\mathcal{V}$ should overestimate the facilitation between far apart strings and over-estimates D. In contrast, a unreasonably small $\mathcal{V}$ would underestimate the population $f(m;\phi_v\mathcal{V})$ of coupled voids and under-estimates D.

A close examination of the comparison between analytic theory and kinetic Monte Carlo simulations in Figs. 5 and 6 reveals that quantitative deviations in D, α and P_{ret} all become more significant for $1/T \gtrsim 4$. This can be improved by increasing $\mathcal{V}$ from 25 to 81, for example, but the fit at higher T then deteriorates. This is consistent with m^* and hence $\mathcal{V}$ expected to increase with $1/T$ as explained above.

VI. LIQUID AND GLASSY LIMITS

For a better intuitive understanding, we now examine asymptotic cases at which simpler analytic expressions can be derived. At high T, all allowed hops are energetically possible so that $q = 1$, as can be illustrated explicitly in Eq. (8). Then, Eq. (18) implies $c_m = m(z-1) \gg 1$ for $m \geq 1$. Alternatively, for large ϕ_v, most regions have $m \simeq \phi_v\mathcal{V} \gg 1$ voids. Then, we have $c_m = m(z-1)q \gg 1$ for not too small values of T and hence q. As a result, for both cases, we have $c_m - 1 \simeq c_m$. Note that the -1 term describes descending the tree level and corresponds to revisiting old configurations. Its diminished importance immediately implies the restoration of simple random walks of both the voids and the particles in the physical space. Using Eq. (23), Eq. (22) gives a diffusion coefficient in the liquid phase as

$$D_{liq} \simeq \frac{z\tilde{l}\tilde{w}a^2\phi_v\Omega}{2d(1 - \phi_v\Omega)}. \quad (27)$$

It follows a simple Arrhenius T dependence at constant ϕ_v inherent from that of $\tilde{w}$. As small ϕ_v, it reduces to

$$D_{liq} \simeq \frac{z\tilde{l}\tilde{w}a^2\phi_v\Omega}{2d}. \quad (28)$$

which implies the power-law in Eq. (4) with a trivial exponent $\alpha = 1$ indicating independent void motions. These qualitative features have been illustrated numerically in the theoretical curves in Fig. 5(a) at large ϕ_v as well as in Fig. 5(b) at high T.

More interestingly, we now consider the glassy limit at low T and small ϕ_v. Terms in Eq. (22) then have

vastly different magnitudes because D_m increases rapidly with m while $f(m;\phi_v\mathcal{V})$ decreases rapidly. Their product maximizes sharply at a particular value of m, say m^* as already suggested in Sec. V.

Physically, m^* is the optimal group size of coupled voids which dominates the dynamics. A maximization of the terms in Eq. (22) after applying Stirling's formula

$$m! \simeq \sqrt{2\pi} m^{m+1/2} e^{-m} \tag{29}$$

gives

$$m^* c_1 - 1 = \frac{2c_1}{\ln(m^*/\phi_v\mathcal{V}) + 1/2m^*}. \tag{30}$$

Neglecting all terms except for $m = m^*$ in Eq. (22), some simple algebra using $e^{-\phi_v\mathcal{V}} \simeq 1$ and Eqs. (18), (29) and (30) gives the diffusion coefficient in the glassy limit as

$$D_{glass} = \frac{l\tilde{w}a^2\Omega c_1 \left(e\phi_v\mathcal{V}/m^*\right)^{m^*}}{2\sqrt{2\pi}d\mathcal{V}\sqrt{m^*}[\ln(m^*/\phi_v\mathcal{V}) + 1/2m^*]}. \tag{31}$$

Since $c_1 \ll 1$ at low T, a simple approximate solution of m^* from Eq. (30) is

$$m^* \simeq 1/c_1. \tag{32}$$

Substituting it into Eq. (31) leads finally to

$$D_{glass} = \frac{l\tilde{w}a^2\Omega c_1^{3/2} \left(e\phi_v\mathcal{V}c_1\right)^{1/c_1}}{2\sqrt{2\pi}d\mathcal{V}\ [\ln(1/\phi_v\mathcal{V}c_1) + c_1/2]}. \tag{33}$$

We find numerically that D_{glass} in Eq. (33) agrees with D from Eq. (22) within a factor close to order unity.

To understand how D_{glass} depend on ϕ_v, we neglect weak logarithmic dependences and Eq. (31) reduces to

$$D_{glass} \sim \phi_v^{m^*}. \tag{34}$$

A comparison with Eq. (4) gives

$$\alpha = m^* \simeq 1/c_1 \tag{35}$$

where we have also used Eq. (32). Hence, the scaling exponent α is simply the dominant group size of the coupled voids, as expected from simple chemical kinetics. These groups of voids even at very low density are able to dominate the dynamics due to their higher mobility analogous to the role of pockets of mobile defects in KCM [11, 43].

At constant ϕ_v, we find numerically that D_{glass} exhibits a super-Arrhenius T dependence which is consistent with the Vogel-Fulcher-Tammann empirical form [1] as expected for glass. Moreover, D_{glass} admits its T dependence via $\tilde{w}$ and c_1. In particular, the factor c_1^{1/c_1} is the main contributor to the super-Arrhenius slow-down. The precise T dependence of D_{glass} is relatively model dependent. For the DPLM with a uniform interaction energy distribution g defined in Eq. (2), it is easy to show using Eqs. (8) and (11) that $c_1 \sim q \sim T^3$ at low T. At constant ϕ_v and neglecting the relatively weak non-exponential dependences, we get a super-Arrhenius form

$$D_{glass} \sim \exp[-(E_0 + bT^{-2})/k_BT] \tag{36}$$

where b is approximately a constant. In general, other system may exhibits other dependences of c_1 on T. One should also consider the dependence of ϕ_v on T, which may be Arrhenius in the simplest cases. This can generates a variety of T dependences of D_{glass} and may account for different fragility observed in glasses [44].

VII. SUMMARY

We have derived a microscopic theory of glassy dynamics based on string-like hopping motions in the presence of disorder quenched in the configuration space of distinguishable particles. The elementary motions are assumed to be micro-strings, which are the synchronize parts of string-like particle hopping motions. A micro-strings is enabled by a void and its propagation transports its associated void from one of its ends of to the other. Voids can be coupled via spatially overlapping micro-strings which interact by mutually enabling or disabling each other, noting that micro-string propagations alter the local energy landscape. The configuration space of a local region with m coupled voids is organized as a graph by identifying particle configurations as nodes and micro-string propagations as edges. The graph can be approximated by the Bethe lattice. Energetically accessible configurations constitute a random tree embedded in the Bethe lattice.

We have analyzed the dynamics in terms of the equivalent pictures of random walks of the local configurations in the random configuration trees, random walks of the voids in the physical space, and random walks of the particles in the physical space. At high temperature T, the random trees can be infinite and voids are fully mobile exhibiting liquid-like behaviors. As T decreases, more micro-strings become energetically unlikely. Random trees for single-void regions becomes finite implying trapping. By contrast, analogous random trees for regions with multiple voids have more children per node due to facilitated dynamics between voids. They can remain infinite implying mobile coupled voids. The dynamics are dominated by coupled voids of a group size m^*, which increases as T decreases. The increasing rarity of these larger dominant groups is responsible for the super-Arrhenius dynamics and kinetic arrest.

Explicit expressions for the particle diffusion coefficient D and the particle hopping return probability P_{ret} are derived. At low void density ϕ_v, the calculated D exhibits super-Arrhenius T-dependence typical of glasses. It also reproduces a scaling law between D and ϕ_v. The scaling exponent α increases continuously as T decreases and is identified as the group size of the coupled voids dominating the dynamics. In addition, our expression for P_{ret}

shows a convergence towards unity at low T as observed previously in both polymer MD and DPLM simulations.

The theory is applied to the DPLM. Using only one tunable parameter $\mathcal{V}$ related to the interaction range of micro-strings, our analytical expressions agree well with measurements from kinetic Monte Carlo simulations of the DPLM from Ref. [27] over a wide range of temperature and void density. Such a direct and detailed quantitative check of a dynamical theory with a model of glass defined in a finite-dimensional physical space is in our knowledge unprecedented. Noting that the DPLM possesses a natural and generic definition and exhibits an extensive range of glassy properties, the agreement provides a solid support of the applicability of our theory to glasses exhibiting string-like hopping motions.

VIII. ACKNOWLEDGMENTS

We thank O.K.C. Tsui, Kai-Ming Lee, Haiyao Deng, and Ho-Kei Chan for helpful discussions, and Chun-Shing Lee for technical assistance. We are grateful to the support of Hong Kong GRF (Grant 15301014).

[1] K. Binder and W. Kob, *Glassy materials and disordered solids: An introduction to their statistical mechanics* (World Scientific, 2011)
[2] M. D. Ediger and P. Harrowell, J. Chem. Phys. **137**, 080901 (2012)
[3] G. Biroli and J. P. Garrahan, J. Chem. Phys. **138**, 12A301 (2013)
[4] F. H. Stillinger and P. G. Debenedetti, Annu. Rev. Condens. Matter Phys. **4**, 263 (2013)
[5] G. Adam and J. H. Gibbs, J. Chem Phys. **43**, 139 (1965)
[6] W. Gőtze, *Complex dynamics of glass-forming liquids: a mode-coupling theory* (Oxford University Press, 2008)
[7] T. R. Kirkpatrick, D. Thirumalai, and P. G. Wolynes, Phys. Rev. A **40**, 1045 (1989)
[8] G. H. Fredrickson and H. C. Andersen, Phys. Rev. Lett. **53**, 1244 (1984)
[9] R. G. Palmer, D. L. Stein, E. Abrahams, and P. W. Anderson, Phys. Rev. Lett. **53**, 958 (1984)
[10] F. Ritort and P. Sollich, Adv. Phys. **52**, 219 (2003)
[11] J. P. Garrahan, P. Sollich, and C. Toninelli, in Dynamical Heterogeneities in Glasses, Colloids and Granular Media, edited by L. Berthier, G. Biroli, J.-P. Bouchaud, L. Cipelletti, and W. van Saarloosand (Oxford University Press, 2011)
[12] C. Donati, J. F. Douglas, W. Kob, S. J. Plimpton, P. H. Poole, and S. C. Glotzer, Phys. Rev. Lett. **80**, 2338 (1998)
[13] M. Aichele, Y. Gebremichael, F. Starr, J. Baschnagel, and S. Glotzer, J. Chem Phys. **119**, 5290 (2003)
[14] Y. Gebremichael, M. Vogel, and S. C. Glotzer, J. Chem. Phys. **120**, 4415 (2004)
[15] E. R. Weeks, J. C. Crocker, A. C. Levitt, A. Schofield, and D. A. Weitz, Science **287**, 627 (2000)
[16] C.-H. Lam, J. Chem. Phys. **146**, 244906 (2017)
[17] H. Miyagawa, Y. Hiwatari, B. Bernu, and J. Hansen, J. Chem. Phys. **88**, 3879 (1988)
[18] K. Vollmayr-Lee, J. Chem. Phys. **121**, 4781 (2004)
[19] M. Vogel, Macromolecules **41**, 2949 (2008)
[20] T. Kawasaki and A. Onuki, Phys. Rev. E **87**, 012312 (2013)
[21] J. W. Ahn, B. Falahee, C. D. Piccolo, M. Vogel, and D. Bingemann, J. Chem. Phys. **138**, 12A527 (2013)
[22] J. Helfferich, F. Ziebert, S. Frey, H. Meyer, J. Farago, A. Blumen, and J. Baschnagel, Phys. Rev. E **89**, 042603 (2014)
[23] W. Kob and H. C. Andersen, Phys. Rev. E **48**, 4364 (1993)
[24] M. Newman and C. Moore, Phys. Rev. E **60**, 5068 (1999)
[25] R. K. Darst, D. R. Reichman, and G. Biroli, J. Chem. Phys. **132**, 044510 (2010)
[26] N. B. Tito, J. E. Lipson, and S. T. Milner, Soft Matter **9**, 3173 (2013)
[27] L.-H. Zhang and C.-H. Lam, Phys. Rev. B **95**, 184202 (2017)
[28] Ajay and R. G. Palmer, J. Phys. A **23**, 2139 (1990)
[29] S.-i. Sasa, Phys. Rev. Lett. **109**, 165702 (2012)
[30] D. Osmanović and Y. Rabin, J. Stat. Phys. **162**, 186 (2016)
[31] L. S. Shagolsem, D. Osmanović, O. Peleg, and Y. Rabin, J. Chem. Phys. **142**, 051104 (2015)
[32] L. S. Shagolsem and Y. Rabin, J. Chem. Phys. **144**, 194504 (2016)
[33] T. S. Ingebrigtsen and H. Tanaka, J. Phys. Chem. B **120**, 7704 (2016)
[34] S. Swayamjyoti, J. Löffler, and P. M. Derlet, Phys. Rev. B **89**, 224201 (2014)
[35] A. S. Keys, L. O. Hedges, J. P. Garrahan, S. C. Glotzer, and D. Chandler, Phys. Rev. X **1**, 021013 (2011)
[36] D. Turnbull and M. H. Cohen, J. Chem. Phys. **34**, 120 (1961)
[37] F. W. Starr, S. Sastry, J. F. Douglas, and S. C. Glotzer, Phys. Rev. Lett. **89**, 125501 (2002)
[38] J. Conrad, F. W. Starr, and D. Weitz, J. Phys. Chem. B **109**, 21235 (2005)
[39] A. Widmer-Cooper and P. Harrowell, J. Non-Cryst. solids **352**, 5098 (2006)
[40] M. Newman, *Networks: an introduction* (OUP Oxford, 2010)
[41] D. Cassi, Euro. Phys. Lett. **9**, 627 (1989)
[42] B. D. Hughes and M. Sahimi, J. Stat. Phys. **29**, 781 (1982)
[43] P. Harrowell, Phys. Rev. E **48**, 4359 (1993)
[44] C. A. Angell, Science **267**, 1924 (1995)